1987

A Review of Mathematical Modeling of the Zinc/Bromine Flow Cell and Battery

T. I. Evans
Texas A & M University - College Station

Ralph E. White
University of South Carolina - Columbia, white@cec.sc.edu

Publication Info

Journal of the Electrochemical Society, 1987, pages 2725-2733.

DOI: 10.1149/1.2100277
http://dx.doi.org/10.1149/1.2100277

24. D. C. Boyd and D. C. Thompson, in "Kirk-Othmer Encyclopedia of Chemical Technology," Vol. 11, 3rd ed., p. 830, John Wiley and Sons, Inc., New York (1980).
25. J. O'M. Bockris and A. K. M. S. Huq, *Proc. R. Soc. London Ser. A*, **237,** 277 (1956).
26. "International Critical Tables," Vol. 7, McGraw-Hill, Inc., New York (1930).
27. D. I. MacDonald and J. R. Boyack, *J. Chem. Eng. Data*, **14,** 380 (1969).
28. G. Scatchard, *Phys. Z.*, **33,** 32 (1932).
29. R. H. Stokes and R. A. Robinson, *J. Am. Chem. Soc.*, **70,** 1870 (1948).
30. P. Zelenay, M. A. Habib, and J. O'M. Bockris, *Langmuir*, **2,** 393 (1986).
31. E. A. Moelwyn-Hughes, "Physical Chemistry," 2nd ed., p. 347, Pergamon Press, Ltd., Oxford (1978).
32. D. E. C. Corbridge, "Phosphorous, An Outline of Its Chemistry, Biochemistry and Technology," 3rd ed., p. 652, Elsevier Pub. Co., Amsterdam (1985).
33. E. A. Moelwyn-Hughes, "Phosphorous, An Outline of Its Chemistry, Biochemistry and Technology," 3rd ed., p. 1030, Elsevier Pub. Co., Amsterdam (1985).
34. V. Jovancicevic, P. Zelenay, and B. R. Scharifker, Unpublished results (1986).
35. E. Yeager, D. Scherson, and B. Simic-Glavaski, in "The Chemistry and Physics of Electrocatalysis," J. D. E. McIntyre, M. J. Weaver, and E. Yeager, Editors, p. 241, The Electrochemical Society Softbound Proceedings Series, Pennington, NJ (1984).
36. B. E. Conway, "Modern Aspects of Electrochemistry," 16, 103 (1985).
37. J. O'M. Bockris and A. Gochev, *J. Phys. Chem.*, **90,** 5232 (1986).
38. D. B. Sepa, M. V. Vojnovic, L. M. Vracar, and A. Damjanovic, *Electrochim. Acta*, **31,** 91 (1986).
39. J. O'M. Bockris and D. C. Lowe, *Proc. R. Soc. London, Ser. A*, **226,** 423 (1954).
40. K. Klinedinst, J. A. S. Bett, J. MacDonald, and P. Stonehart, *J. Electroanal. Chem. Interfacial Electrochem.*, **57,** 281 (1974).
41. A. Wieckowski and M. Szklarczyk, *ibid.*, **142,** 157 (1982).
42. H. S. Frank and M. W. Evans, *J. Chem. Phys.*, **13,** 507 (1945).
43. M. J. Weaver, *J. Phys. Chem.*, **83,** 1748 (1978).
44. P. Wetterholm, Personal communication through R. Parsons.

A Review of Mathematical Modeling of the Zinc/Bromine Flow Cell and Battery

T. I. Evans* and R. E. White**

Department of Chemical Engineering, Texas A&M University, College Station, Texas 77843

ABSTRACT

Mathematical models which have been developed to study various aspects of the zinc/bromine cell and stack of cells are reviewed. Development of these macroscopic models begins with a material balance, a transport equation which includes a migration term for charged species in an electric field, and an electrode kinetic expression. Various types of models are discussed: partial differential equation models that can be used to predict current and potential distributions, an algebraic model that includes shunt currents and associated energy losses and can be used to determine the optimum resistivity of an electrolyte, and ordinary differential equation models that can be used to predict the energy efficiency of the cell as a function of the state of charge. These models have allowed researchers to better understand the physical phenomena occurring within parallel plate electrochemical flow reactors and have been instrumental in the improvement of the zinc/bromine cell design. Suggestions are made for future modeling work.

The zinc/bromine (Zn/Br_2) flow battery has received much interest as a rechargeable power source because of its good energy density, high cell voltage, high degree of reversibility, and abundant low cost reactants (1-4). Problems with the Zn/Br_2 battery include high cost electrodes, material corrosion, the formation of dendrites during zinc deposition on charge, high self-discharge rates, unsatisfactory energy efficiency, and relatively low cycle life (400-600 cycles) (2, 4, 5). Experimental and modeling efforts have been conducted to alleviate these problems.

Several companies, including Energy Research Corporation (ERC), Gould, and Exxon have developed this battery by building and testing various designs (1). The Exxon design (3, 6-8), which uses a corrosion resistant carbon-plastic composite material for the electrodes, a separator, and a second liquid phase to complex the bromine in the electrolyte to prevent it from participating in the self-discharge reaction, effectively deals with most of the problems mentioned earlier. The main concerns at present are to improve battery efficiency and increase cycle life (1, 2) without sacrificing the attractive low cost of the battery. The experimental approach for obtaining the design variables and operating conditions that yield acceptably high efficiencies and cycle lives can be time consuming and costly. Modeling the system can reduce the experimentation required by pointing out to the experimenter the independent design parameters and how they can be changed to better the cell performance.

* Electrochemical Society Student Member
** Electrochemical Society Active Member.

Several mathematical models of the Zn/Br_2 cell and a mathematical model of a stack of cells have been presented (4, 9-14). These models have provided researchers with a means to study the various aspects of the Zn/Br_2 cell and gain a greater understanding of the physical phenomena affecting the performance of this battery. The models by Lee and Selman (9), Evans and White (14), and Van Zee *et al.* (12) provide predictions for many aspects of the Zn/Br_2 cell and battery of interest to designers. These predictions include the current density distributions along the electrode surfaces, the overall battery efficiency, and round trip cell efficiencies. The models reviewed here are all steady-state models and macroscopic in nature. Microscopic models which focus on dendrite initiation and growth during electrodeposition have also been presented (15-17) with one model by Lee (11) which combines a macroscopic model (9) of the Zn/Br_2 flow reactor with a microscopic model describing dendrite growth. These microscopic models, which have contributed much to the understanding of dendrite growths and to the steps which can be taken to reduce their adverse effects, are kept separate from the macroscopic models addressed here and have already been discussed elsewhere (11).

Models of the Zn/Br_2 cell and a stack of cells are based on the recirculation system shown in Fig. 1 and on the parallel plate geometry of an individual cell shown in Fig. 2. Aqueous electrolyte solutions containing reactive species (see Table I for a typical feed composition) are stored in external tanks and circulated through each cell in the stack. Each cell contains two electrodes at which

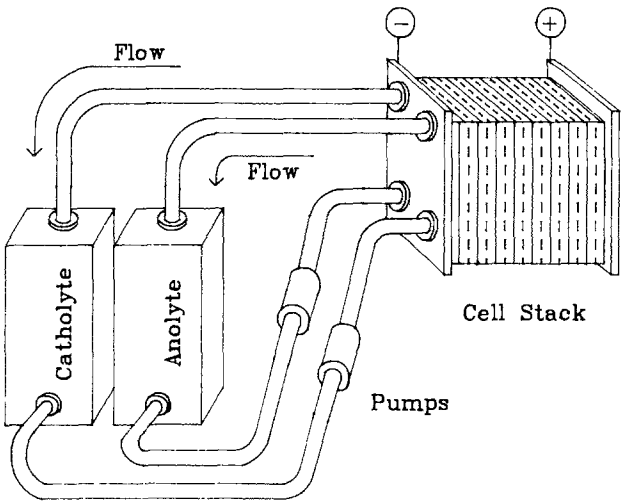

Fig. 1. Schematic of a Zn/Br_2 flow battery

reversible electrochemical reactions occur. Sometimes, a porous layer or flow-through porous region is used for the bromine electrode (not shown in Fig. 2). The electrochemical reactions that are assumed to occur (2-4) are, at the bromine electrode

$$2Br^- \rightleftharpoons Br_2 + 2\,e^- \quad [1]$$

and at the zinc electrode

$$Zn^{2+} + 2e^- \rightleftharpoons Zn \quad [2]$$

To charge the battery, either a constant voltage or a constant current is applied to the stack and energy is stored as Zn and Br_2. During charge, the reduction of bromine

$$Br_2 + 2e^- \rightarrow 2Br^- \quad [3]$$

at the zinc electrode is an undesired side reaction which competes with zinc deposition and is important to include in the modeling (13). The gap between the positive and negative electrodes, in which electrolyte flows, is usually divided by a porous separator to prevent Br_2 from reaching the zinc electrode where it participates in the undesirable reaction [3]. A second liquid phase, organic and known as the "red oil" phase in the Exxon design (3, 6-8), is circulated with the electrolyte to capture bromine and further prevent it from reaching the zinc electrode. The organic phase contains complexing agents like quaternary ammonium salts with which the bromine associates to form an emulsion (2). This emulsion, which is insoluble in water and has a different density than water, travels with the aqueous electrolyte to the storage tank where it is gravitationally separated. Thus, the bromine is effectively stored. In the bulk aqueous electrolyte solution, complexation of Br^- and Br_2 to form tri-bromide ions (Br_3^-) occurs (18) according to

$$Br_2 + Br^- \rightleftharpoons Br_3^- \quad [4]$$

In addition, zinc ions can react with bromide in the electrolyte to form several different zinc-bromine complexes (19-21)

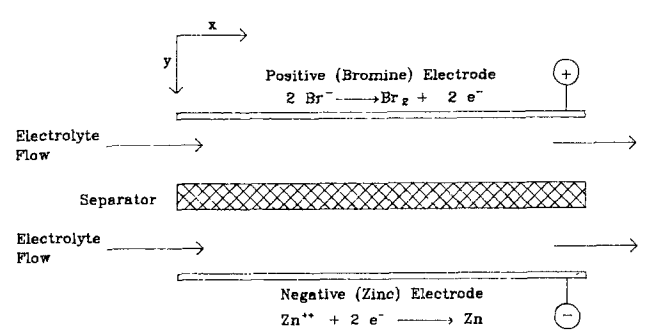

Fig. 2. Schematic of the Zn/Br_2 cell modeled by Putt (4), Lee and Selman (9, 10), Lee (11), and Mader and White (13).

Table I. A typical initial electrolyte composition of a Zn/Br_2 flow cell

Species (i)	$C_{i,\,feed}$[a] $(mol/cm^3) \times 10^3$
Na^+	1.000
Br^-	2.949
Br_2	0.001
Zn^{2+}	1.000
Br_3^-	0.051

[a] Feed to each channel is assumed equal (3, 13). Electrolyte concentrations in the two channels will change differently as charging proceeds due to their separation.

$$Zn^{2+} + Br^- \rightleftharpoons ZnBr^+ \quad [5]$$

$$Zn^{2+} + 2Br^- \rightleftharpoons ZnBr_2 \quad [6]$$

$$Zn^{2+} + 3Br^- \rightleftharpoons ZnBr_3^- \quad [7]$$

$$Zn^{2+} + 4Br^- \rightleftharpoons ZnBr_4^{2-} \quad [8]$$

Other species, in addition to those listed in Table I and which appear in reactions [5]-[8], probably exist as postulated by Hsie *et al.* (19, 20). The extent to which these zinc species are present and influence cell performance is assumed negligible in all of the models (4, 9-14) pesented so far. Discharge occurs when the battery is connected to a load and the backward directions of reactions [1] and [2] take place at the positive and negative electrodes, respectively.

Discussion

The models of the Zn/Br_2 electrochemical reactor (4, 9-14) have been developed to understand the physical phenomena occurring and to determine how cell performance can be improved. These models have been used to investigate the relative importance of the species transport, electrokinetics, cell geometry, operating conditions, secondary electrode reactions, and chemical reactions in the electrolyte bulk on cell performance. Key design considerations such as the thickness of the separator, the initial electrolyte concentration, the electrolyte flow rate, the applied cell potential or current, and the thickness of the porous bromine electrode have been addressed by the various models. Model developments have shown which quantities and groups of quantities are the independent adjustable parameters of the cell and model predictions have shown how these parameters can be adjusted to improve cell performance. The model by Putt (4) was developed to provide a rational approach for optimizing the Gould design and for later scale-up. A similar model, developed by Lee and Selman (9), is used to examine the effects of certain design parameters on the current density distribution along the electrode surfaces. Lee (11) extended Lee and Selman's model (9) to obtain the approximate time dependent behavior of the current density distribution. He went on to link his macroscopic model with a microscopic model, describing the growth of zinc dendrites, to determine how to reduce dendrite growth rates in the flow system. Van Zee *et al.* (12) have developed a simplified model of the entire Zn/Br_2 battery to determine how overall efficiency can be increased by changing certain design conditions. The models by Mader and White (13) and Evans and White (14) are similar to the models of Putt (4) and Lee and Selman (9) but make different simplifying assumptions. Their models attempt to include as many of the cell features in the model as is possible because of the belief that a detailed model will yield the most realistic and useful predictions for use by cell designers. As the Zn/Br_2 battery technology has progressed, the need to model different aspects of this battery has arisen. For example, the dendrite problem has been one of the major obstacles in the development of a viable Zn/Br_2 system, therefore prompting the work of Putt (4) and Lee (11). These models (4, 9-14), with their different predictive capabilities, have been developed to meet the changing needs in the development of the Zn/Br_2 system and to

provide a sound theoretical basis for future development of this battery.

The following equations form the basis for the models to be discussed. The material balance equation for species i is

$$\frac{\partial c_i}{\partial t} = -\nabla \cdot \mathbf{N}_i + R_i \qquad [9]$$

Since all of the models discussed here are steady-state models, the accumulation term ($\partial c_i/\partial t$) is set equal to zero. Using dilute solution theory (22), the flux of species i ($\mathbf{N}_i$) may be written as

$$\mathbf{N}_i = \mathbf{v}c_i - D_i\nabla c_i - z_i\frac{D_i}{RT}\mathbf{F}c_i\nabla\Phi \qquad [10]$$

where the three terms on the right-hand side of Eq. [10] represent convection, diffusion, and migration, respectively. The term R_i, in Eq. [9], represents production of species i due to chemical reaction and is used, for example, to account for the complexing of the bromine, reaction [4]. The production of species due to electrochemical reactions that occur at the flat electrodes is incorporated into the boundary conditions of the models. These electrochemical reactions are usually assumed to follow a Butler-Volmer type rate expression (23)

$$i_j = i_{oj,ref}\left\{\prod_i(\theta_{i,o})^{p_{ij}}\exp\left(\frac{\alpha_{aj}\mathbf{F}}{RT}\eta_j\right) - \prod_i(\theta_{i,o})^{q_{ij}}\exp\left(\frac{-\alpha_{cj}\mathbf{F}}{RT}\eta_j\right)\right\} \qquad [11]$$

where i_j is the faradaic current density due to electrochemical reaction j, $\theta_{i,o}$ is the dimensionless local surface concentration of species i, and η_j is the local overpotential (*i.e.*, the potential driving force for the electrochemical reaction j)

$$\eta_j = V - \Phi_o - U_{j,ref} \qquad [12]$$

For those models considering only one reaction at each electrode, i_j in Eq. [11] is simply equal to i, the total faradaic current density.

Each model is presented by explaining its origin, purpose, governing equations, and important predictions and their relation to the design of the Zn/Br_2 system. The thin diffusion layer models [*i.e.*, the models of Putt (4), Lee and Selman (9, 10), and Lee (11)] are discussed first. The battery model presented by Van Zee *et al.* (12) is reviewed next, followed by a review of the recent models of Mader and White (13) and Evans and White (14). Table II gives a summary comparison of the features included in these models.

Thin diffusion layer models.—The models by Putt (4), Lee and Selman (9, 10), and Lee (11) are sometimes referred to as thin diffusion layer models (24). They include the assumption that the concentrations of the species in the flow channels remain constant, over the channel gaps and entire reactor length, except within thin diffusion layers adjacent to the electrode surfaces. This simplifying assumption was first introduced in a model of a parallel plate electrochemical reactor by Parrish and Newman (25) and seems reasonable for low conversions per pass. However, White *et al.* (24) have pointed out the shortcomings of this assumption, especially the fact that models which include this assumption cannot predict the conversion per pass of a reactant. Hence, many cell performance criteria important to cell designers such as cell efficienices, as defined by Mader and White (13), cannot be determined with the thin diffusion layer models.

For these models, Eq. [9] and [10] are simplified for the electrolyte bulk and diffusion layers as follows. For the electrolyte bulk, Eq. [9] and [10] reduce to the two-dimensional Laplace equation

$$\nabla^2\Phi(x, y) = 0 \qquad [13]$$

since uniform composition is assumed. For the thin diffusion layers, the migration of species is assumed negligible, relative to convection and diffusion. This assumption is based on Levich's (26) work which showed that the migration term can be neglected when excess supporting electrolyte is present. This assumption and the assumption that no homogeneous reactions occur are used to reduce Eq. [9] and [10] to the well known convective diffusion equation (22)

$$v_x\frac{\partial c_i}{\partial x} = D_i\frac{\partial^2 c_i}{\partial y^2} \qquad [14]$$

To calculate Φ within the thin diffusion layers, Eq. [13] must then be used. As White *et al.* (24) have pointed out, this use of Eq. [13] may have little effect on the predicted potential in the diffusion layers but because the overall effect may be significant, the electrochemical reaction rate depends exponentially on the solution potential.

The models of Putt (4) and Lee and Selman (9) have been used to investigate methods of smoothing the current density distribution along the negative (zinc) electrode surface. During charge, and under certain operating conditions such as a high charging rate, the deposited metal may exhibit areas of roughness as well as protrusions. The worst case of such nonuniform deposition is the formation and growth of long needle-like metallic protrusions called dendrites. Due to spherical diffusion to the dendrite tip, among other factors, dendrites can rapidly propagate, reaching deeper into the electrolyte, and may even span the gap between the elec-

Table II. A comparison of the macroscopic models of the Zn/Br_2 flow system ("Yes" indicates inclusion and "No" indicates exclusion of feature)

Model author(s) (Ref.)	Entire recirculation system	Shunt current protection	Pumping energy	Terminal effect	Separator	Porous bromine electrode	Reaction [3]	Reaction [4]	Discharge	No. of dimensions
R. Putt (4)	No	No	Yes[a]	Yes	Yes	Yes	No	No	No	2
Lee and Selman (9)	No	No	No	Yes	Yes	No	No	No	No	2
Lee and Selman (10)	No	No	No	No	Yes	No	No	No	No	2
Lee (11)	Yes	No	No	Yes	Yes	No	No	No	No	2
Van Zee *et al.* (12)	Yes	Yes	Yes	No	Yes	No	No	No	Yes	1
Mader and White (13)	No	No	No	No	Yes	No	Yes	Yes	No	2
Evans and White (14)	No	No	No	No	Yes	Yes	Yes	Yes	Yes	2

Features not yet included in a model:
1. Zinc complexation reactions in the bulk electrolyte.
2. A bromine-rich second phase circulated with the electrolyte.
3. Time dependence (*i.e.*, the dynamic problem).

[a] Calculation is separate from model.

trodes and short the cell. Also dendrites may cause separator damage and may result in decreased cell capacity due to loss of active material (17). It has been reported that the dendrite problem is more severe at higher current densities (4). Hence, it is desirable to have a uniform current density distribution so that there are no localized areas having current densities substantially higher than the average. The models by Putt (4) and Lee and Selman (9) can be used to provide the design criteria for achieving the optimum current density distribution.

Putt's model, which is limited to the charge half cycle, can be used to predict the current and potential distributions along the electrodes given the total current to the cell, electrode dimensions, electrode and electrolyte conductivities, and the electrode kinetic parameters. The model consists of a set of algebraic, integral, and partial differential equations which are solved iteratively. The cell geometry considered is the same as that shown in Fig. 2. Putt used this geometry even though his positive electrode was a flow-through porous electrode (4).

Putt's model is based on Eq. [9] and [10] and on conservation of charge. The separator is treated as a region of electrolyte whose dimensions are such that its ionic resistivity is that of the separator (*i.e.*, the concept of an "effective separator thickness" is used). The terminal connections are located on the electrodes at the electrolyte exits (*i.e.*, trailing ends). The kinetics of the zinc electrode and the porous bromine electrode are assumed to obey the linear form of the Butler-Volmer equation for flat plate electrodes

$$i = \beta\eta \qquad [15]$$

The iterative solution procedure begins by using guesses of the faradaic current densities $i_2(x)$ and $i_3(x)$, where $i_2(x)$ is the current density in the electrolyte adjacent to the negative electrode and $i_3(x)$ is the current density in the electrolyte adjacent to the positive electrode. Conservation of charge is applied at the negative and positive electrodes to obtain the electronic current densities $i_1(x)$ and $i_4(x)$, respectively. For example, conservation of charge for the negative electrode is written as

$$i(x) = \frac{-I}{S_{NE}W} - \frac{\int_0^x i_2(x)dx}{S_{NE}} \qquad [16]$$

The electrode potentials, $\Phi_1(x)$ and $\Phi_4(x)$, are calculated from $i_1(x)$ and $i_4(x)$ using Ohm's law for the electrodes given the ionic resistivity of the electrode material and the porosity of the porous positive electrode. That is, to account for the porous nature of the positive electrode, Putt divided the electronic current density, $i_4(x)$, by the porosity to calculate $\Phi_4(x)$. Laplace's equation, Eq. [13], is used to calculate the solution potential, Φ. Once Φ_1, Φ_4, and Φ have been calculated, the overpotential at each electrode is calculated according to Eq. [12]. A concentration overpotential term (22) is included in the calculation of the overpotential for the negative electrode to account for the effect of the limited mass transfer of the Zn^{2+} ions to the electrode surface where they undergo reduction to zinc. An analytical solution to Eq. [14] is used to obtain the concentration of the zinc ions at the electrode surface and this concentration is then used to calculate the concentration overpotential. Next, Eq. [15] is used to obtain new estimates of the faradaic current density distributions, $i_2(x)$ and $i_3(x)$. The calculation process is repeated until successive estimates of $i_2(x)$ and $i_3(x)$ differ by less than some prescribed tolerance.

Putt used his model to determine the important design criteria for smoothing the current density distribution along the negative electrode surface. Lowering zinc bromide concentration, increasing the channel gaps, using thicker electrodes, and impeding the electrode kinetics (by lowering the value of β in Eq. [15]) and mass transfer (by decreasing the zinc ion diffusion coefficient) are methods which were shown to achieve relatively smooth current density distributions. A current density of 40 mA/cm² and an electrode length of 30.48 cm were input into the model to obtain the results reported. Minimums in the current density distributions were detected at distances approximately 13% from the leading edge (where the electrolyte enters) to the trailing edge (where the electrolyte exits) of the electrode. It is at this position where the combined effects of concentration polarization and electrode resistance seem to have the most influence.

Some simplifying assumptions made in the development of Putt's model should be questioned. The linear form of the Butler-Volmer equation used by Putt applies only at small values of the overpotential. This assumption becomes invalid when overpotentials are necessarily large during high rate charging. The porous bromine electrode should not be treated as a flat plate electrode because the electrokinetics and mass transport in both cases will be substantially different. Evans and White (14), for example, have shown that it is important to include the electrokinetic and mass-transfer effects within the porous layer in the modeling. Concerning the solution technique, Putt notes that his iterative scheme becomes erratic at times and thus convergence to the solution may be difficult for some cases. To handle this convergence problem, Putt used a weighted average of the previous iterate, $i_2(x)_{k-1}$, and the current iterate, $i'_2(x)_k$, to obtain a new guess for $i_2(x)$

$$i'_2(x)_k = (0.98)\, i_2(x)_{k-1} + (0.02)\, i_2(x)_k \qquad [17]$$

Thus, only small changes in successive iterates result and it is resonable to assume that the convergence is quite slow in some instances.

Similar to Putt's model, Lee and Selman's (9) model was developed to predict current density distributions and, in particular, to determine the effects of the separator and terminal resistances on these distributions. The geometry considered is the parallel plate design shown in Fig. 2. The current densities and reactant concentrations along the positive and negative electrodes as well as the current density in the separator as a function of the dimensionless axial (x-direction) distance are calculated given the cell dimensions, operating conditions, kinetic parameters, and physical constants. The model consists of integral and algebraic equations which are solved using orthogonal collocation.

The governing equations for Lee and Selman's model are developed from Eq. [9] and [10]. Transport of species in the separator is assumed to occur by migration only and Ohm's law is used to describe the current-potential relationship in the separator. Equations [13] and [14] are used to obtain the solution potential and the reactant concentration profiles in the thin diffusion layers, respectively. As in Putt's model, the terminal effect is accounted for by using the current balance, Eq. [16], and subsequently using Ohm's law for the electrodes to relate the electronic current density to the electrode potential. Lee and Selman incorporated Ohm's law for the electrode directly into the derivative of Eq. [16] to obtain the following equation

$$\frac{d^2V(x)}{dx^2} = -\frac{i(x)}{\kappa_e S_E} \qquad [18]$$

Using boundary conditions consistent with the common assumptions of thin diffusion layer models, analytical solutions have been obtained for Eq. [13], [14], and [18]. Lee and Selman used these analytical solutions, which are integral equations involving the current density, in their model to calculate the two-dimensional (x, y) electrolyte potential profile, the one-dimensional (x) reactant concentration profile, and the one-dimensional (x) electrode potential profile. Ohm's law for the separator is used to relate the solution potential on either border of the separator to the current density in the separator

$$\Phi_{sep,C}(x) - \Phi_{sep,A}(x) = -\frac{S_s}{\kappa_{sep}} i_{sep}(x) \qquad [19]$$

Equation [11] is used to calculate electrochemical reaction rates at the electrode surfaces. A concentration overpotential term is included in Eq. [12] as in Putt's work.

An overall current balance, which states that the total current passing through the anode must also pass through the separator and then through the cathode, is used to complete the equation set. The dimensionless equations are solved using orthogonal collocation.

The dimensionless parameters in Lee and Selman's model which were found to govern the current density distributions are T, i_o^*, and R_t, for each flow channel, and the quantities ψ, R_c, R_s, and $<i^*>$, for the cell. T and i_o^* represent the ratio of electrical resistance to mass-transfer resistance in the electrolyte and the ratio of mass-transfer resistance to kinetic resistance, respectively. R_c represents the mass-transfer effect in one channel relative to the other channel, and ψ is a dimensionless ratio of cell length to channel gap. The parameters R_t and R_s characterize the terminal and separator effects, respectively. Lee and Selman (9) describe R_t as a measure of the electrical resistance of an electrode relative to the mass-transfer resistance in the particular flow channel. Similarly, R_s can be thought of as a measure of the electrical resistance of the separator, relative to the mass-transfer resistance. Lee and Selman show that there exists an optimum value for R_t for a given average current density. High and low values of R_t result in very nonuniform current density distributions. High values of R_s were shown to smooth the current density distribution but at the expense of the cell potential. The ratio of average current density to the smallest average limiting current density, $<i^*>$, was found to be the most important parameter affecting the current density distribution. In general, smoother current density distributions were obtained from the model for lower values of $<i^*>$.

By changing these dimensionless parameters in their model, Lee and Selman discovered several significant features about the current density along the electrodes. When terminal effects are appreciable and the current collector tab is mounted on the electrodes at the electrolyte entrance, the current density is highest at this point and continually decreases away from the terminals as expected. However, if the current collector tab is mounted at the trailing end of the electrode and terminal resistance is appreciable, the current distribution along the electrode surface becomes more level with a minimum current density occurring between the entrance and trailing ends of the electrode. This observation agrees with Putt's findings. In addition, when both terminal effects and separator resistance are considered, the current distribution is further smoothed almost to the point where a plot of current density *vs.* axial distance is a straight horizontal line [see Fig. 2 in (9)]. The model is used to show that, if the current collector tabs are properly located, then cells operating at high rates (*i.e.*, at relatively large current densities) do not necessarily display current maldistribution along the electrodes, as is often thought to be the case. Also, the model predictions also show that there exists a flow velocity and reactant concentration in each channel which optimizes the current distribution for the characteristics of the given electrode reaction. Lastly, cell dimensions and applied potential were found to influence strongly the average current density, as confirmed and studied in detail by Mader and White (13).

Lee and Selman's (9) model is more complete than Putt's model in the sense that fewer simplifying assumptions are made. For example, the terminal tabs are not assumed to be located at the cell exit ends, the separator is treated as a separate cell region and not as an "effective" span of electrolyte, and Eq. [11] as opposed to Eq. [15] is used. However, in Lee and Selman's model, the assumption that transport occurs by migration only in the separator may lead to large errors when significant concentration differences exist between the anolyte and catholyte, giving rise to a large diffusion contribution to the flux there. The models of Putt (4) and Lee and Selman (9) may be used to test the assumption of constant current density along the electrode surfaces made in the development of other parallel plate electrochemical reactor models (10-14, 27-29).

Lee and Selman's (9) model has been extended by Lee (11) to obtain estimates of the time dependent behavior of the Zn/Br_2 cell. Such predictions are useful because it is important to know how the cell performance changes over time. For example, it is desirable to keep the energy efficiency of the system near its optimum value throughout the discharge, and have it drop off only at the very end of the discharge. Lee (11) considered an entire half-cell system, either the positive flow channel and its corresponding anolyte storage tank or the negative flow channel and its corresponding catholyte storage tank. Time propagation is simulated by running consecutive steady-state cases, as was done by Lee *et al.* (30) in earlier work.

Lee modified the steady-state model (9) to include conditions which govern the changes occurring over successive time intervals. Two overall material balances, one on the cell channel and one on the corresponding storage tank, are combined to yield the following expression for the concentration change with time

$$c_{t_2} = c_{t_1} + \frac{LW}{V_{st}}(t_2 - t_1)\left[\frac{<i>_{t_1}}{nF} + <N_{sep}>_{t_1}\right] \quad [20]$$

In Eq. [20], $<i>$ is the average current density calculated from the current density distribution obtained from the steady-state model (9) at the conditions of time t_1. $<N_{sep}>$ is the flux of the species entering the channel from the separator. This quantity is estimated using the average transference number of the species and the separator current density obtained from the steady-state model (9) at time t_1. For the catholyte channel, Lee also accounted for the changing thickness of the zinc deposit as time progresses, its influence on the electrolyte velocity in the channel, and its subsequent effect on the concentration profile in the thin diffusion layer.

Lee (11) used his model to show several time dependent effects of the design criteria on cell performance. He showed that the average cell current will degrade faster when the cell is operated at higher applied voltages. Near the end of charge, as reactant concentrations dwindle and polarization becomes severe, increasing flow velocity was shown to prolong cell life (*i.e.*, by sustaining the average current density at a fairly high level) because it improves the mass transfer of the reactants. Also, the unevenness of the zinc deposit was found to become quite considerable (*e.g.*, 40 μm differences) after long periods of charging (*e.g.*, 6h).

A thin diffusion layer model for predicting corrosion rates in compartmented flow cells, as shown in Fig. 2, has also been presented by Lee and Selman (10). The model is used to study the corrosion rate of zinc during charge by the reaction product of the positive electrode, bromine. The model consists of a set of algebraic and partial differential equations which are solved analytically to yield a set of integral equations. Equations [9] and [10] are used to determine the concentration distribution of the corrosive species (Br_2 in the Zn/Br_2 flow cell), thus the corrosion rate. Concentration changes are assumed to vary linearly in the separator from the anolyte bulk concentration to the catholyte bulk concentration. In the separator, transport is assumed to occur by diffusion only. The governing equations in the flow channels are simply

$$C_{b,A} = \text{a constant (specified)} \quad [21]$$

$$C_{b,C} = \text{a constant (calculated)} \quad [22]$$

where C represents the concentration of the corrosive species and subscripts b, A, and C, indicate the bulk, anolyte, and catholyte, respectively. In the separator, the flux of the corrosive species is

$$N_{sep} = D_{sep}\frac{C_{b,A} - C_{b,C}}{S_s} \quad [23]$$

Equation [14] applies in the thin diffusion layer adjacent to the zinc electrode surface. The kinetics for the corro-

sion reaction are assumed to be given by a pseudo first-order rate expression

$$R'_i = kC_o \qquad [24]$$

where C_o is the concentration of the corrosive species at the electrode surface. This reaction is assumed to be relatively insensitive to changes in potential because it is assumed that the corrosion potential would be much closer to the zinc reaction (reaction [2]) equilibrium potential than to the bromine reaction (reaction [1]) equilibrium potential due to the relatively high exchange current density of reaction [2] and because of the mass-transfer resistance of bromine toward the zinc electrode. The algebraic and partial differential equations resulting from these assumptions are solved analytically using boundary conditions consistent with the assumptions stated above and using the superposition principle (31). The integral equations which result are solved to obtain the concentration profile of the corrosive species and thus the corrosion rate.

Lee and Selman (10) found that two dimensionless parameters, K_1 and K_2, govern the corrosion rate and its distribution along the cathode in their model. K_1 represents the ratio of mass-transfer resistance in the catholyte channel to kinetic resistance of the corrosion process at the zinc electrode. K_2 represents the ratio of diffusion resistance in the separator to kinetic resistance of the corrosion process at the zinc electrode. The concentration of the corrosive species is plotted *vs.* K_1 and K_2, and it is shown that corrosion is at a minimum for large values of K_2 and small values of K_1. Using an experimentally determined diffusion coefficient for bromine and an estimated value for k in Eq. [24], an average zinc corrosion rate in a typical Zn/Br_2 flow cell was determined to be about 1 mA/cm^2.

This corrosion current density value seems reasonable for open-circuit conditions, but it is unlikely that zinc corrodes on charge because zinc is being deposited. That is, the corrosion reaction of zinc

$$Zn(s) + Br_2(aq) \rightarrow Zn^{2+}(aq) + -Br^-(aq) \qquad [25]$$

requires that zinc metal enter the solution which does not happen on charge. This is illustrated in Fig. 3 where it is shown that the difference between the potential of the zinc electrode and the adjacent solution ($V_c - \Phi_o$) is less than the open-circuit potential for the zinc electrode ($U_{Zn,ref}$). This must be true, otherwise zinc would not be deposited. Thus, on charge, zinc is deposited and bromine is reduced, as shown in Fig. 3 by points A and B, respectively. These arguments assume that $V_c - \Phi_o$ is the same everywhere over the zinc surface, whereas there may exist regions of differing potential, perhaps below $U_{Zn,ref}$. The authors believe that these regions do not contribute significantly to the overall kinetics and that the foregoing arguments hold true. However, it should be pointed out that this matter is still under investigation (32, 33).

Finally, significant disagreement between the concentration profile of the corrosive species proposed by Lee and Selman (10) in Fig. 2 of their paper and the concentration profile of Br_2 in Fig. 8 of Evans and White (14) suggests that the bulk electrolyte concentrations should not be treated as constants. This suggestion applies to all the thin diffusion layer models. Also, the anolyte bulk concentration is a set quantity in Lee and Selman's model (10). The feed concentration is more appropriately used as a known quantity and the steady-state concentration profile is a quantity to be calculated.

An algebraic Zn/Br_2 battery model.—Van Zee *et al.* (12) presented a simple algebraic model of Exxon's design (3, 6-8) of the Zn/Br_2 battery which can be used to predict the energy efficiency of the battery for various electrolyte resistivities and cell dimensions. This model is used to help select design parameters to minimize the energy losses in the battery due to pumping the electrolyte and due to the protective energy required to reduce shunt currents. The model includes the recirculation system,

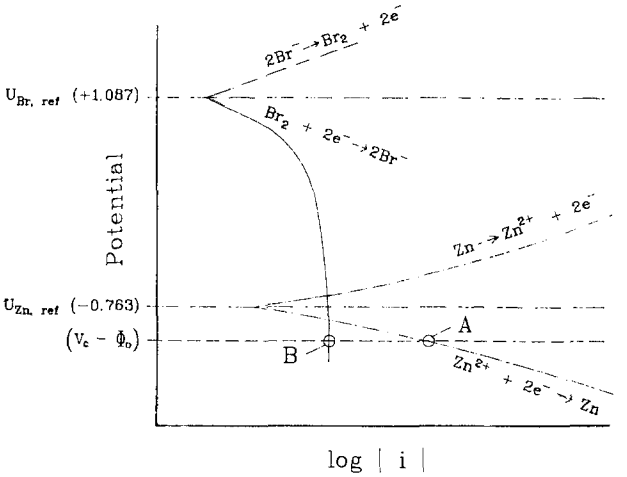

Fig. 3. Polarization plot showing cathodic protection of zinc electrode during charge. (Not to scale, potentials given are relative to H_2 electrode.)

as shown schematically in Fig. 1, and is based on the cell geometry shown in Fig. 2.

Van Zee *et al.* (12) calculate the energy efficiency of the Zn/Br_2 battery as

$$\eta_E = \frac{E_c - (E_{SD} + E_{PD})}{E_I + E_{SC} + E_{PC}} \qquad [26]$$

where E_c is the energy capacity of the battery, E_I is the input energy to the battery, E_{SD} and E_{SC} are the protective energies required to minimize shunt current losses during discharge and charge, respectively, and E_{PD} and E_{PC} are the pumping energies during discharge and charge, respectively. Ohm's law is used to calculate E_c and E_I, given the appropriate current densities and estimated cell resistance. The cell resistance is calculated by multiplying the electrolyte resistance by the sum of the effective electrolyte thicknesses of the anolyte channel, separator, and catholyte channel. This "effective thickness" concept was used earlier by Putt (4) to account for the higher resistance offered by the separator relative to the surrounding electrolyte. Van Zee *et al.* (12) used effective thicknesses for three regions of the cell to account for the "tortuosity" and "porosity" of each region. The equations for E_{SD} and E_{SC} are derived for the system using Kirchoff's loop and node rules and are given by Grimes *et al.* (7). E_{PD} and E_{PC} are determined based on calculated pressure drops and an assumed pump efficiency. The algebraic set of equations which result from the analysis are solved in sequence given the cell dimensions, physical properties, and operating conditions.

Van Zee *et al.* (12) used their model to show that the energy efficiency of the Zn/Br_2 battery is a complicated function of the electrolyte resistivity and electrolyte channel width when all other geometric parameters and physical properties are specified. They showed that a maximum energy efficiency (79.6%) exists at a certain electrolyte resistivity (5.5 Ω-cm) for a given channel width (0.062 in.). Also, the the model is used to show that an optimal separator thickness exits for a given set of design criteria.

The model presented by Van Zee *et al.* (12) is useful for obtaining rough estimates of energy efficiencies for an entire Zn/Br_2 battery, but it is of limited utility for the design of an individual Zn/Br_2 flow cell. The model is based on the assumption of constant electrolyte resistivity throughout charge and discharge, whereas this property would change as the concentrations of the species change. The transport taking place inside the cell is treated in an approximate manner; for example, the tortuosity and porosity are arbitrarily specified. The kinetics of the electrochemical reactions are not included in the model.

Other Zn/Br_2 cell models.—Mader and White (13) and Evans and White (14) present mathematical models for

the Zn/Br_2 flow cell which predict the performance of the cell as a function of the cell dimensions and operating conditions. The model by Evans and White (14) is an extension of the model by Mader and White (13). Both models follow the modeling approach outlined by White *et al.* (24). Performance criteria of interest to cell designers, such as conversions per pass and total cell efficiency on charge, are defined by Mader and White and are calculated based on predicted concentration and potential distributions. Like the previously discussed models, these two models were developed to aid in understanding the physical phenomena occurring within the Zn/Br_2 cell and to determine ways of improving cell efficiency. The models attempt to account for as many of the cell features as is possible because of the belief that "detailed" models offer the most realistic and, hence, useful predictions for battery development. Also such models can be used to study the many aspects of the system and how they interact to affect overall performance.

The governing equations are the mass balance for each species, Eq. [9], in two dimensions and the electroneutrality condition

$$\sum_i c_i z_i = 0 \qquad [27]$$

Equation [10] is used to describe the flux of each species in the flow channels. In the separator, the convection term in Eq. [10] is neglected and effective diffusivities are used. In the channels, the species mass balances are simplified by deleting certain partial derivative terms because they can be shown to be small relative to the other terms in the equation. Specifically, when the aspect ratio ($\alpha = S/L$) is small, the diffusion and migration terms of the flux expression in the x (axial) direction are negligible relative to the diffusion and migration terms in the y (radial) direction as demonstrated by Nguyen *et al.* (27). Equation [11] is used to describe the electrode kinetics. The homogeneous, chemical reaction [4] is included in both models and is assumed to be at equilibrium according to the equilibrium constant given by Eigen and Kustin (18)

$$K_{eq} = \frac{c_{Br_3^-}}{c_{Br^-}\, c_{Br_2}} = 17 M^{-1} \qquad [28]$$

The parasitic reduction of bromine at the zinc electrode, reaction [3], is also accounted for in both models. The resulting dimensionless equations are solved by using the finite difference technique and Newman's BAND(J) subroutine (22, 34). The solution technique is an iterative one and requires reasonable initial guesses of the unknowns (the dimensionless concentration of each species, θ_i, and the solution potential, Φ). The kinetic parameters used in both models were obtained by Mader (35) by fitting model predictions to the current density data in the literature (3).

Mader and White used their model to show the effects of the design criteria on cell performance. The independent adjustable design parameters in Mader and White's model were found to be the residence time of the electrolyte in the cell (L/v_{avg}), the flow channel width (S_A), the effective separator thickness ($N_m S_S$), and the applied cell potential (E_{cell}). These independent parameters are used as input to the model, the equation set is solved for the unknowns (θ_i, Φ), and performance criteria (*e.g.*, coulombic efficiency, voltaic efficiency, total efficiency, and conversion per pass) are calculated. Coulombic efficiency is a measure of the fraction of current which passes through the zinc electrode and produces the desired zinc deposition, reaction [2], as opposed to the parasitic bromine reduction, reaction [3]. Voltaic efficiency is the ratio of the theoretical potential necessary for charging the cell to the actual applied potential. The product of the coulombic and voltaic efficiencies is the total efficiency. Not only are performance criteria determined at the initial state of charge, but they are calculated at states of charge ranging from 0% Zn^{2+} plated to about 35% Zn^{2+} plated. The percent Zn^{2+} plated is a quantity used to follow the state of charge (3) and is calculated using the conversion per pass of Zn^{2+} as described by Mader (35). The state of charge is changed by running consecutive steady-state cases and using the average output concentrations from one run as the feed concentrations for the next run. A similar approach (*i.e.*, consecutive steady states) was used earlier by Lee (11) to approximate the time dependent behavior of the cell. Mader and White found that cell efficiency decreases as the effective separator thickness increases at the initial state of charge. However, larger effective separator thicknesses yield high cell efficiencies at later states of charge. Also, residence time was shown to have a small effect on cell efficiency.

Their model is useful because it can be used to predict product conversions and energy efficiencies for a separated cell having multiple electrode reactions. However, the model neglects several features of the physical system as shown in Table II. It should be noted that Mader and White (13) did not consider the terminal effect in their model, but that this feature could be added by using the current balance of Lee and Selman (9), Eq. [18], as a boundary condition, and treating the electrode potential as an unknown.

Evans and White (14) augmented the model presented by Mader and White to include a thin porous layer on the bromine electrode (see Fig. 4), the capability to generate predictions for the discharge half cycle, and the ability to make predictions for constant current operating conditions. The model can be used to calculate design criteria, as defined by Mader and White, for both the charge and discharge half cycles. Evans and White define a round trip energy efficiency which can be calculated from the predictions for any given charge/discharge cycle.

The governing equations of this model include those used in the work of Mader and White and the equations used to describe the porous bromine electrode. The material balance equation for species i in the porous layer is Eq. [9] where the production term, R_i, is replaced by

$$R_i = R^\circ_i + R'_i \qquad [29]$$

R°_i is the production of species i due to reaction in the electrolyte within the pores (homogeneous reaction) and R'_i is the rate of production of species i due to the electrochemical reactions that the species may be involved in on the pore surfaces (heterogenous reaction) and is given by

$$R'_i = -\sum_j \frac{a\, s_{ij}\, i_j}{n_j \mathbf{F}} \qquad [30]$$

In Eq. [30], a is the specific electroactive surface area of the porous material and i_j is the current density, due to electrochemical reaction j based on the electroactive surface area within the porous electrode. i_j is calculated using Eq. [11]. Since convective transport is assumed to be negligible in the porous region, Eq. [10] without the convection term is used to calculate the flux of each species within the porous layer.

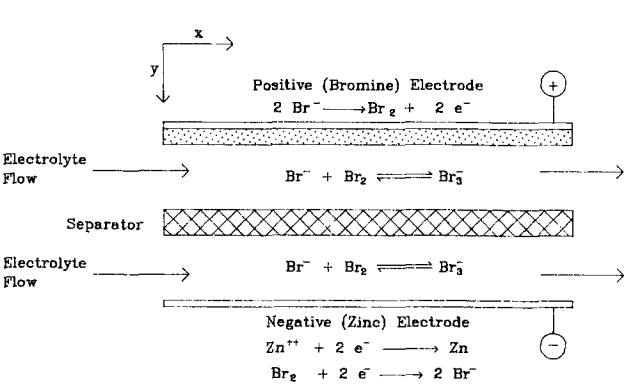

Fig. 4. Schematic of the Zn/Br_2 cell modeled by Evans and White (14).

Evans and White used their model to determine the effects of the mass transfer and electrokinetics in the porous bromine electrode on the round trip performance of the cell. They found that increasing the porous bromine electrode thickness increased the cell efficiency. The model predictions, for the kinetic parameters used, showed that reaction controlled conditions existed where diffusion of reactive species into and out of the porous electrode was virtually uninhibited. The independent adjustable parameters in Evans and White's model were determined to be the residence time of electrolyte in the cell (L/v_{avg}), the flow channel width (S_A), the MacMullin number of the separator material (N_m), the thickness of the separator (S_S), the thickness of the porous electrode (S_{PE}), the MacMullin number of the porous electrode ($N_{m,PE}$), the specific surface area of the porous electrode material (a), and, either the applied cell potential (E_{cell}), or the applied current density (i_n). For the porous electrode thicknesses investigated, the predictions showed that greater round trip energy efficiencies result for thicker porous electrodes. Evans and White show that round trip energy efficiencies of about 70% should be possible for the Zn/Br_2 cell.

Evans and White's model is perhaps the most complete of all the cell models discussed in that it accounts for many features of the cell and does not require many of the simplifying assumptions made in the development of the other models (4, 9-12). For example, the assumptions of constant bulk concentrations, no homogeneous chemical reactions, and no diffusion contribution to the flux in the separator. The model can be used to determine the effects of the design criteria on cell performance for a full charge/discharge cycle. The kinetic parameters used, as mentioned earlier, were taken from the work of Mader and White (13) and are listed in Table II of that paper. Other kinetic parameters may produce a diffusion limited condition, which may also be of interest. Given experimental results from a working cell, the model should provide an excellent means of determining certain system parameters such as diffusivities, D_i, and electrokinetic constants, $i_{oj,ref}$, a_{aj}, and a_{cj}. The model would have to be embedded within a parameter estimation scheme, such as ZXSSQ in the IMSL software library (36), so that model predictions could be fitted to the experimental data by finding the "best" values for these system parameters. Unfortunately, very little experimental data for the Zn/Br_2 system is currently available.

Summary and Recommendations

Models of the Zn/Br_2 flow cell have been used to show the important design criteria for improving cell performance. The models of Putt (4), Lee and Selman (9, 10), and Lee (11) have provided important information for improving current density distributions. The model by Van Zee *et al.* (12) has been used to show how certain design parameters can be changed to achieve an optimum overall performance for the entire Zn/Br_2 battery system. Mader and White (13) and Evans and White (14) have established many of the independent design parameters for an individual cell and have shown how to improve cell efficiency, via changes in these design criteria.

Future modeling work of the Zn/Br_2 battery should include features not yet accounted for by existing models. For example, the model by Evans and White (14) should be extended to include zinc complexing (reactions [5]-[8]), a second bromine-rich phase, time dependence (*i.e.*, the dynamic problem), and a self-contained recirculation system consisting of a cell, the two electrolyte storage tanks, and the connecting piping.

Acknowledgment

The authors would like to thank the reviewers of this manuscript for their valuable comments and inputs.

Manuscript submitted July 29, 1986; revised manuscript received June 8, 1987.

LIST OF SYMBOLS

a	specific electroactive surface area of the porous electrode, cm^{-1}
c_i	concentration of species i, mol/cm^3
$c_{i,ref}$	reference concentration of species i, mol/cm^3
$C_{b,A}$	concentration of corrosive species in the anolyte bulk, $kmol/m^3$
$C_{b,C}$	concentration of corrosive species in the catholyte bulk, $kmol/m^3$
C_o	concentration of corrosive species at the electrode surface, $kmol/m^3$
D_i	diffusion coefficient of species i, cm^2/s
D_{sep}	effective diffusivity of the corrosive species in the separator, m^2/s
E_{cell}	applied cell potential ($= V_a - V_c$), V
E_c	energy capacity of the battery not including auxiliaries, J
E_I	energy input to battery not including auxiliaries, J
E_{pC}	energy required for pumping electrolyte on charge, J
E_{pD}	energy required for pumping electrolyte on discharge, J
E_{SC}	energy required for shunt current protection on charge, J
E_{SD}	energy required for shunt current protection on discharge, J
$\mathbf{F}$	Faraday's constant, 96,487 C/mol
I	total cell current, A
i	current density, A/m^2
$\mathbf{i}$	current density vector, A/m^2
i_{sep}	current density in separator, A/m^2
i_j	current density due to electrochemical reaction j
i_n	total current density at zinc electrode ($= I/LW$), A/cm^2
$i_{oj,ref}$	exchange current density of electrochemical reaction j, A/cm^2
i_1	electronic current density in negative electrode, A/cm^2
i_4	electronic current density in positive electrode, A/cm^2
i_2	faradaic current density at the surface of the negative electrode, A/cm^2
i_3	faradaic current density at the surface of the positive electrode, A/cm^2
$<i>$	average current density, A/cm^2
$<i^*>$	average dimensionless current density
k	first-order electrochemical reaction rate constant, m/s
K_{eq}	equilibrium constant for tri-bromide reaction, cm^3/mol
L	electrode length, cm
L/v_{avg}	residence time of the reactor, s
$\mathbf{N}_i$	flux vector of species i, $mol/(cm^2 \times s)$
N_{sep}	flux of corrosive species through separator, $mol/(m^2s)$
$<N_{sep}>$	flux of species entering the channel from the separator, $mol/(m^2s)$
N_m	MacMullin number in the separator
$N_{m,PE}$	MacMullin number in the porous electrode
$N_m S_S$	effective separator thickness, cm
p_{ij}	anodic reaction order of species i in reaction j
q_{ij}	cathodic reaction order of species i in reaction j
R	gas law constant, $8.314\ J/(mol \times K)$
R_i	production rate of species i due to reaction, $mol/(cm^3 \times s)$
R°_i	production rate of species i due to homogeneous reaction, $mol/(cm^3 \times s)$
R'_i	production rate of species i due to electrochemical reaction, $mol/(cm^3 \times s)$
S	total electrode gap, cm
S_A	anolyte channel width, cm
S_E	thickness of the electrode, m
S_{NE}	thickness of the negative electrode, cm
S_{PE}	thickness of the porous electrode, cm
S_S	thickness of the separator, cm
T	temperature, K
t	time, s
$U_{j,ref}$	open-circuit potential of reaction j based on the reference concentrations, V
$\mathbf{v}$	velocity vector, cm/s
v_{avg}	average velocity of the electrolyte, cm/s
v_x	flow velocity, cm/s
V	electrode potential, V
V_a	anode potential, V

V_c cathode potential, V
V_{PE} potential at the top of the positive electrode (corresponds to the total cell overpotential, V)
V_{st} volume of the storage tank, cm^3
W width of the electrode, cm
x axial coordinate, cm
y radial coordinate, cm
z_i charge number of species i

Greek

α aspect ratio, S/L
α_{aj} anodic transfer coefficient for reaction j
α_{cj} cathodic transfer coefficient for reaction j
β electrokinetic parameter in the linear Butler-Volmer equation, $A/(cm^2\ V)$
ϵ porosity of porous electrode material
η_E energy efficiency of the battery including auxiliaries
η overpotential for reaction at the electrode surface, V
η_j overpotential for reaction j at electrode surface ($V_e - \Phi_{oe} - U_{j,ref}$), V
$\theta_{i,o}$ dimensionless concentration of species i ($c_i/c_{i,ref}$) at electrode surface
κ_e conductivity of electrode, mho/m
κ_{sep} conductivity of separator, mho/m
ρ_{PE} ionic resistivity of the porous electrode substrate, (Ω cm)
Φ_o solution potential at electrode surface, V
$\Phi_{sep,A}$ potential of electrolyte at separator/anolyte border, V
$\Phi_{sep,C}$ potential of electrolyte at separator/catholyte border, V
Φ_1 potential in the negative electrode, V
Φ_4 potential in the positive electrode, V

REFERENCES

1. J. L. Chamberlin, in "Proceedings of the EPRI/LBL Workshop on the Electrochemistry of Zinc/Halogen Batteries," Palo Alto, CA, Nov. 30-Dec. 1, 1983, Vol. I, p. 2-15 (1984).
2. W. J. Walsh and P. C. Symons, "Transfer of Battery Technology Developed by the U.S. Department of Energy," ANL/SPG-25, Argonne National Laboratory, Argonne, IL (1984).
3. R. Bellows, P. Grimes, H. Einstein, E. Kantner, P. Malachesky, and K. Newby, *IEEE Trans. on Veh. Tech.*, **VT-32,** 26 (1983).
4. R. Putt, "Assessment of Technical and Economic Feasibility of Zinc/Bromine Batteries for Utility Load-Levelling," EPRI report EM-1059, project 635-1, Palo Alto, CA, Appendix M (1979).
5. L. Nanis, "Zinc-Bromine Battery Workshop Summary," EPRI, Palo Alto, CA (1978).
6. R. Bellows, in "Proceedings of the EPRI/LBL Workshop on the Electrochemistry of Zinc/Halogen Batteries," Palo Alto, CA, Nov. 30-Dec. 1, 1983, Vol. I, p. 4-3 (1984).
7. P. Grimes, R. Bellows, and M. Zahn, in "Electrochemical Cell Design," R. E. White, Editor, p. 259, Plenum Publishing Co., New York, (1984).
8. P. Grimes and R. Bellows, in "Electrochemical Cell Design," R. E. White, Editor, p. 227, Plenum Publishing Co., New York (1984).
9. J. Lee and J. R. Selman, *This Journal,* **129,** 1670 (1982).
10. J. Lee and J. R. Selman, *ibid.*, **130,** 1237 (1983).
11. J. Lee, Ph.D. Dissertation, Illinois Institute of Technology, Chicago, IL (1981).
12. J. W. Van Zee, R. E. White, P. Grimes, and R. Bellows, in "Electrochemical Cell Design," R. E. White, Editor, p. 293, Plenum Publishing Co., New York (1984).
13. M. J. Mader and R. E. White, *This Journal,* **133,** 1297 (1986).
14. T. I. Evans and R. E. White, *ibid.*, **134,** 866 (1987).
15. J. L. Barton and J. O'M Bockris, *Proc. R. Soc. London, Ser. A,* **268,** 485 (1962).
16. J. W. Diggle, A. R. Despić, and J. O'M Bockris, *This Journal,* **116,** 11 (1969).
17. U. Landau and J. H. Shyu, "Roughness Evolution and Dendrite Growth in Zinc Electrodeposition From Halide Electrolytes," EPRI report EM-2937, project 1198-3, Palo Alto, CA, (1983).
18. M. Eigen and K. Kustin, *J. Am. Chem. Soc.,* **84,** 1355 (1962).
19. W. C. Hsie, M. L. Gopikanth, and J. R. Selman, *Electrochim. Acta.*, **30,** 1371 (1985).
20. W. C. Hsie and J. R. Selman, *ibid.*, **30,** 1381 (1985).
21. P. Grimes, Exxon Research, personal communications.
22. J. S. Newman, "Electrochemical Systems," Prentice-Hall, Inc., Englewood Cliffs, NJ (1973).
23. R. E. White, S. E. Lorimer, and R. Darby, *This Journal,* **130,** 1123 (1983).
24. R. E. White, M. Bain, and M. Raible, *ibid.*, **130,** 1037 (1983).
25. W. R. Parrish and J. S. Newman, *ibid.*, **117,** 43 (1970).
26. V. G. Levich, "Physiochemical Hydrodynamics," Prentice-Hall, Inc., Englewood Cliffs, NJ (1962).
27. T. V. Nguyen, C. W. Walton, R. E. White, and J. W. Van Zee, *This Journal,* **133,** 81 (1986).
28. T. V. Nguyen, C. W. Walton, and R. E. White, *ibid.*, **133,** 1136 (1986).
29. M. J. Mader, C. W. Walton, and R. E. White, *ibid.*, **133,** 1124 (1986).
30. J. Lee, R. Selman, and H. Shimotake, "Design and Optimization of the Lithium/Ion Sulfide Cell Electrodes. Bi-monthly Report," ANL-CENI-8019, Argonne National Laboratory, Argonne, IL (1980).
31. F. G. Hildebrand, "Advanced Calculus for Applications," Prentice-Hall, Englewood Cliffs, NJ (1962).
32. S. L. Chiu and J. R. Selman, in "Electrochemical Engineering Applications," AIChE Symposium Series, Vol. 83, p. 15, New York (1987).
33. S. L. Chiu and J. R. Selman, in "Electrochemical Engineering Applications" AIChE Symposium Series, Vol. 83, p. 111, New York (1987).
34. R. E. White, *Ind. Eng. Chem. Fundam.*, **17,** 367 (1978).
35. M. J. Mader, M. S. Thesis, Texas A&M University, College Station, TX (1985).
36. IMSL, "The IMSL Users Manual," IMSL Library, Vol. 1 (1984).